

dependent interstellar chemical model¹², adapted to the cometary conditions (details will be published elsewhere¹³; see also Fig. 3 legend). We find that HCN undergoes proton transfer from H_3O^+ to produce HCNH^+ , which can in turn react by proton transfer with H_2CO and NH_3 , or by dissociative recombination with electrons to give HNC (and HCN). Dissociative recombination is the most important pathway according to our calculations. Although there are a number of somewhat uncertain parameters in the model, the similar production and destruction pathways for HNC and HCN make the calculated HNC/HCN ratio rather insensitive to most of these parameters. For example, we find that varying the initial (nuclear) abundances of various nitrogen-containing species over a wide range ($0 < \text{N}_2 < 0.3$; $0.002 < \text{NH}_3 < 0.05$, relative to H_2O) has little effect on the HNC/HCN ratio.

The parameters crucial to the calculated HNC/HCN ratio are the branching ratios for the principal HNC production route, $\text{HCNH}^+ + e$. There are no laboratory measurements of these ratios, and the standard values used for interstellar chemistry assume that this dissociative recombination yields $\text{HCN}:\text{HNC}:\text{CN}$ in the ratios 0.25:0.25:0.5 (ref. 14). However, very recent quantum-chemical calculations suggest that the production of HNC should exceed that of HCN and that little CN will be produced¹⁵. This is consistent with the conclusions from extensive observations of HCN and HNC isotopomers in the interstellar medium, from which the branching ratios are deduced to be¹⁶ $\text{HCN}:\text{HNC}:\text{CN} = 0.4:0.6:0$. We adopt here the slightly more conservative ratios $\text{HCN}:\text{HNC}:\text{CN} = 0.45:0.55:0$.

The results of this chemical model are plotted in Fig. 3. The model matches the observations very well, both in terms of the maximum value of the HNC/HCN ratio and in terms of the dependence of this ratio on heliocentric distance r . The nonlinear character of the dependence on r seems to be a result of the multi-stage chemical process which produces HNC and the density-squared dependence of the bimolecular reactions involved.

A source for HNC from the CHON grains^{17,18} in the coma might involve multiple processes which could conceivably mimic the observed heliocentric dependence, and can perhaps not be completely ruled out. However, we feel that HNC in Hale-Bopp must be produced in significant measure by gas-phase, ion-molecule chemistry initiated by the photoionization of H_2O . A similar conclusion has been reached with an independent chemical model by Rodgers and Charnley¹⁹, and our chemical model also predicts an abundance and coma distribution of HCO^+ in agreement with the observations¹¹. We conclude that HNC is, to our knowledge, the first neutral cometary molecule whose existence in active comets can be ascribed in large part to chemical processes in the coma. As a corollary, it follows that in such comets the effects of chemistry in the coma must be included in deducing the original composition of the nucleus. □

Received 9 October 1997; accepted 30 March 1998.

- Irvine, W. M. *et al.* Spectroscopic evidence for interstellar ices in comet Hyakutake. *Nature* **383**, 418–420 (1996).
- Lovas, F. J. Recommended rest frequencies for observed interstellar molecular microwave transitions—1991 revision. *J. Phys. Chem. Ref. Data* **21**, 181–271 (1992).
- Bockele'e-Morvan, D., Padman, R., Davies, J. K. & Crovisier, J. Observations of submillimeter lines of CH_3OH , HCN, and H_2CO in comet P/Swift-Tuttle with the James Clerk Maxwell Telescope. *Planet. Space Sci.* **42**, 655–662 (1994).
- Lovell, A. J. *et al.* HCO⁺ imaging of comet C/1995 O1 Hale-Bopp. *Astrophys. J. Lett.* **497**, L117–L121 (1998).
- Wink, J. *et al.* Evidence for extended sources and temporal modulations in molecular observations of C/1995 O1 (Hale-Bopp) at the IRAM interferometer. *Earth Moon Planets Abstr.* (in the press).
- Biver, N. *et al.* Evolution of the outgassing of Comet Hale-Bopp (C/1995 O1) from radio observations. *Science* **275**, 1915–1918 (1997).
- Biver, N. *et al.* Long-term evolution of the outgassing of comet Hale-Bopp from radio observations. *Earth Moon Planets* (in the press).
- Irvine, W. M. *et al.* In *The Far Infrared and Submillimetre Universe* (ed. Wilson, A.) 277–280 (SP-401, ESA, Noordwijk Netherlands, 1997).
- Notesco, G. & Bar-Nun, A. Trapping of methanol, hydrogen cyanide, and *n*-hexane in water ice, above its transformation temperature to the crystalline form. *Icarus* **126**, 336–341 (1997).
- Tacconi-Garman, L. E., Schloerb, F. P. & Claussen, M. J. High spectral resolution observations and kinematic modeling of the 1667 MHz hyperfine transition of OH in comets Halley (1982i), Giacobini-Zinner (1984e), Hartley-Good (1985i), Thiele (1985m), and Wilson (1986i). *Astrophys. J.* **364**, 672–686 (1990).

- Lovell, A. J. *et al.* HCO⁺ ion-molecule chemistry in comet C/1995 O1 Hale-Bopp. *Earth Moon Planets* (in the press).
- Bergin, E. A. & Langer, W. D. Chemical evolution in pre-protostellar and protostellar cores. *Astrophys. J.* **486**, 316–328 (1997).
- Irvine, W. H. *et al.* Chemistry in cometary comae. *Faraday Discuss.* **109** (in the press).
- Herbst, E. What are the products of polyatomic ion-electron dissociative recombination reactions? *Astrophys. J.* **222**, 508–516 (1978).
- Shiba, Y., Hirano, T., Nagashima, U. & Ishii, K. Potential energy surfaces and branching ratio of the dissociative recombination reaction $\text{HCNH}^+ + e^-$: An *ab initio* molecular orbital study. *J. Chem. Phys.* **108**, 698–705 (1998).
- Hirota, T., Yamamoto, S., Mikami, H. & Ohishi, M. Abundances of HCN and HNC in dark cloud cores. *Astrophys. J.* (in the press).
- Mumma, M. J., Weissman, P. R. & Stern, S. A. in *Protostars and Planets III* (eds Levy, E. H. & Lunine, J. I.) 1177–1252 (Univ. Arizona Press, Tucson, 1993).
- Fomenkova, M. in *From Stardust to Planetesimals* (eds Pendleton, Y. J. & Tielens, A. G. G. M.) 415–421 (ASP Conf. Ser. 122, Astron. Soc. Pacific, San Francisco, 1997).
- Rodgers, S. D. & Charnley, S. B. HNC and HCN in comets. *Astrophys. J. Lett.* (in the press).
- Crovisier, J. Rotational and vibrational synthetic spectra of linear parent molecules in comets. *Astron. Astrophys. Suppl.* **68**, 223–258 (1987).
- Festou, M. C., Rickman, H. & West, R. M. Comets II. Models, evolution, origin and outlook. *Astron. Astrophys. Rev.* **5**, 37–163 (1993).
- Goldsmith, P. F., Langer, W. D., Ellder, J., Irvine, W. M. & Kollberg, E. Determination of the HNC to HCN abundance ratio in giant molecular clouds. *Astrophys. J.* **249**, 524–531 (1981).
- Goldsmith, P. F., Irvine, W. M., Hjalmarson, Å. & Ellder, J. Variations in the HCN/HNC abundance ratio in the Orion molecular cloud. *Astrophys. J.* **310**, 383–391 (1986).
- Olofsson, H., Johansson, L. E. B., Hjalmarson, Å. & Nguyen-Quang-Rieu. High sensitivity molecular line observations of IRC +10216. *Astron. Astrophys.* **107**, 128–144 (1982).
- Schmidt, H. U., Wegman, R., Huebner, W. F. & Boice, D. C. Cometary gas and plasma flow with detailed chemistry. *Comput. Phys. Commun.* **49**, 17–59 (1988).
- Proc. 1st Int. Conf. on Comet Hale-Bopp (to be published as a special issue of *Earth, Moon, Planets*).

Acknowledgements. We thank B. Marsden and D. Tholen for rapidly providing us with the best available cometary elements, and the staff at the JCMT for their assistance with the observations. This work was partly supported by the NSF and NASA.

Correspondence and requests for materials should be addressed to W.M.I. (e-mail: irvine@fcr1.phast.umass.edu).

Electronic liquid-crystal phases of a doped Mott insulator

S. A. Kivelson*, E. Fradkin† & V. J. Emery‡

* Department of Physics, University of California Los Angeles, Los Angeles, California 90095, USA

† Department of Physics, University of Illinois, Urbana, Illinois 61801-3080, USA

‡ Brookhaven National Laboratory, Upton, New York 11973-5000, USA

The character of the ground state of an antiferromagnetic insulator is fundamentally altered following addition of even a small amount of charge¹. The added charge is concentrated into domain walls across which a π phase shift in the spin correlations of the host material is induced. In two dimensions, these domain walls are 'stripes' which can be insulating^{2,3} or conducting^{4–6}—that is, metallic 'rivers' with their own low-energy degrees of freedom. However, in arrays of one-dimensional metals, which occur in materials such as organic conductors⁷, interactions between stripes typically drive a transition to an insulating ordered charge-density-wave (CDW) state at low temperatures. Here it is shown that such a transition is eliminated if the zero-point energy of transverse stripe fluctuations is sufficiently large compared to the CDW coupling between stripes. As a consequence, there should exist electronic quantum liquid-crystal phases, which constitute new states of matter, and which can be either high-temperature superconductors or two-dimensional anisotropic 'metallic' non-Fermi liquids. Neutron scattering and other experiments in the copper oxide superconductor $\text{La}_{1.6-x}\text{Nd}_{0.4}\text{Sr}_x\text{CuO}_4$ already provide evidence for the existence of these phases in at least one class of materials.

Classical liquid crystals⁸ are phases that are intermediate between a liquid and a solid, and spontaneously break the rotation and/or translation symmetries of free space. The proposed electronic liquid crystals are quantum analogues of these phases in which the ground state is intermediate between a liquid, where quantum fluctuations

are large, and a crystal, where they are small. Because the electrons exist in a solid, it is the point-group symmetry of the host crystal that is spontaneously broken, rather than the symmetry of free space. The discussion here will be restricted to a two-dimensional (or quasi-two-dimensional) square lattice, but the generalization to other crystalline symmetries is straightforward. The various zero-temperature phases can then be classified as follows. (1) The liquid phase breaks no spatial symmetries and, in the absence of disorder, is a conductor or a superconductor. (2) The nematic phase breaks the four-fold rotation symmetry of the lattice, but leaves both translation and reflection symmetries unbroken; it is an anisotropic liquid with an axis of orientation. (3) The smectic phase breaks translational symmetry in only one (symmetry) direction. Along the other direction, it has the character of an electron liquid; the smectic order is necessarily commensurate with the underlying lattice at zero temperature. (4) The crystalline phase breaks translation symmetry and has the character of an electronic 'solid'; that is, it is insulating.

We now show how these phases arise, assess their stability, and explore some consequences; at the end we discuss their experimental 'signatures'. We first consider an isolated metallic stripe in a Mott insulator. Such a river of charge is a prototypical example of the one-dimensional electron gas in an active environment⁹, about which much is known. This system is generally 'quantum critical': that is, as the temperature $T \rightarrow 0$, the correlation length diverges and correlation functions fall off as a power of the distance. Frequently there is a gap Δ_s in the spin excitation spectrum, so the only low-energy degrees of freedom are the CDW and the dual superconducting fluctuations whose susceptibilities diverge as $T \rightarrow 0$, as:

$$\chi_{\text{CDW}} \approx \Delta_s T^{-(2-K_c)}; \chi_{\text{SC}} \sim \Delta_s T^{-(2-1/K_c)} \quad (1)$$

where K_c is a non-universal critical exponent¹⁰ which depends on the magnitude and sign of the interactions and satisfies $0 < K_c < 1$ for repulsive interactions.

Direct evidence¹¹⁻¹⁶ of stripe correlations has been obtained over the past few years from neutron-scattering experiments on the copper oxide superconductors, which are the best-studied examples of doped antiferromagnets. It is thus reasonable to ask whether these stripes are relevant for the mechanism of high-temperature superconductivity⁹. Typically, in conventional superconductors, the superconducting gap and transition temperature, T_c , are small because they involve pairing of charged particles, that is, electrons. However, in one dimension, because of the fact that the low-energy excitations are independent spin and charge collective modes¹⁰, superconducting pairing involves only the (neutral) spin degrees of freedom, and hence the gap can be large⁹. This would be a good starting point for a mechanism of high-temperature superconductivity, except for the fact⁷ that higher-dimensional interactions typically lead to CDW order rather than superconductivity because the CDW susceptibility is the more divergent as $T \rightarrow 0$; see equation (1). On the other hand, as we show below, transverse stripe fluctuations have a significant effect on the competition between superconducting and CDW order. Such fluctuations are unimportant in conventional quasi-one-dimensional solids, where there are no background spins to define the meandering rivers of charge, and the constituent molecules, upon which the electrons move, have a large mass. But the zero-point energy $\hbar\omega$ of the transverse stripe fluctuations becomes a significant energy scale in a stripe phase of a doped antiferromagnet which arises from a purely electronic correlation effect. Indeed, we have found that, as $\hbar\omega$ increases in magnitude relative to the Coulomb interaction V , there is a first-order phase transition from an electronic solid to an electronic smectic liquid crystal, in which the CDW fluctuations on neighbouring stripes are uncorrelated at large distances. At the same time, the effective Josephson coupling J between superconducting fluctuations on neighbouring stripes is greatly enhanced as a function of increasing $\hbar\omega/V$.

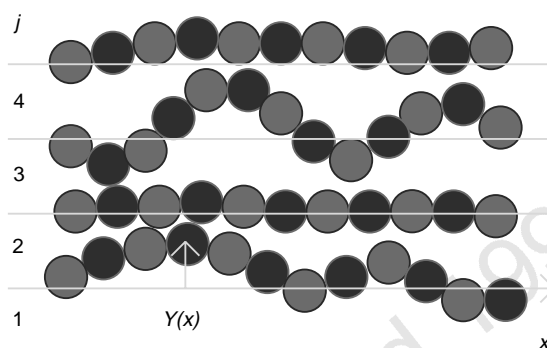


Figure 1 Schematic representation of a smectic stripe phase. The shaded circles represent periodic structures along the stripes, which are forced out of phase by the transverse fluctuations.

We begin with a simple model of a two-dimensional array of stripes along the x direction. In the ordered state, we can safely ignore dislocations and overhangs. This allows us to introduce a coordinate system in which points on the stripes are labelled by a stripe number, j , and by a position x along the stripe direction. Then the stripe configuration is described by the transverse displacement in the y direction, $Y_j(x)$, of the j th stripe at position x (Fig. 1). Because of the spin gap, the only other low-energy degrees of freedom involve fluctuations of the charge density, $\rho_j(x)$, on each stripe. However, because the stripes do not remain straight, the electronic degrees of freedom (holes) sense a fluctuating geometry. Consequently, the local charge density can be expressed as:

$$\rho_j(x) = \bar{\rho} + \rho_0 \cos[\sqrt{2\pi}\phi_j + 2k_F L_j(x)] \quad (2)$$

$$L_j(x) = \int_0^x dx' \sqrt{1 + (\partial_x Y_j)^2} + L_j(0) \quad (3)$$

where $\phi_j(x)$ defines the phase of the CDW with wavevector equal to twice the Fermi wavevector k_F and $L_j(x)$ is the arc-length, that is, the distance measured along the stripe j . The quantum dynamics of this system is equivalent to a theory of the longitudinal (ϕ_j) and transverse (Y_j) vibrations of coupled elastic strings. This defines the hamiltonian for the smectic phase. (A substrate potential would inevitably lock the smectic phase to a wavevector commensurate with the underlying crystal lattice, and hence the transverse modes would be gapped¹⁷.)

The coupling between the CDWs on neighbouring stripes is of the form:

$$H_c = \sum_j \int dx V(\Delta_j Y) \cos[\sqrt{2\pi}(\Delta_j \phi) - 2k_F(\Delta_j L)] \quad (4)$$

plus higher harmonics. Here L_j is defined in equation (3), $\Delta_j F \equiv F_{j+1} - F_j$, and the function $V[\Delta_j Y]$ reflects the fact that CDWs on adjacent stripes are more strongly coupled where the stripes are close together than when they are far apart. When this coupling is strong, it will drive the system into a fully crystalline state. Finally, there is a term in the hamiltonian representing the Josephson tunnelling of (superconducting) pairs of electrons between stripes. The tunnelling matrix element:

$$J(\Delta_j Y) \approx J_0 \exp[-\alpha \Delta_j Y] \quad (5)$$

depends roughly exponentially on the local spacing of the stripes, where α is a constant. The fact that superconductivity is a $k = 0$ order implies that the Josephson coupling does not depend on the arc length L_j , and hence it is not affected by the geometry of the stripes.

With this background, it is possible to state our central point that, to all orders in perturbation theory in powers of V , all terms that are not invariant under the transformation $\phi_j(x, t) \rightarrow \phi_j(x, t) + \delta_j$

(where t is time) for arbitrary δ_j are non-vanishing only near the 'surface', so in the thermodynamic limit the phases ϕ_j of the CDW fluctuations on neighbouring stripes are not locked together and there is no CDW order. The physical origin of this effect is easily understood. The difference in arc lengths, $\Delta_j L = L_{j+1}(x) - L_j(x)$, is a sum of contributions with random sign, which are more or less independently distributed along the distance $|x|$. For this reason, $\Delta_j L$ (and the dephasing) grow with increasing $|x|$ roughly as in a random walk, that is $|\Delta_j L|^2 \sim D|x|$, where D is a transverse diffusion constant.

This result may be obtained formally by integrating out the stripe fluctuations (Y) perturbatively in powers of V and, subsequently, J . To first order in V , the effective interaction between the CDWs on neighbouring stripes, $V^{(1)}(x; \Delta\phi(x))$, is given by the expression:

$$V^{(1)}(x; \Delta\phi) = \langle V(\Delta Y) \cos[\sqrt{2\pi}(\Delta\phi) - 2k_F(\Delta L)] \rangle \quad (6)$$

where $\langle \rangle$ implies averaging over transverse stripe fluctuations. To lowest order in a cumulant expansion:

$$V^{(1)}(x; \Delta\phi) = \bar{V}(x) \cos[\sqrt{2\pi}(\Delta\phi)] \quad (7)$$

$$\bar{V}(x) = \langle V(\Delta Y) \rangle \exp\{-(2k_F^2 \langle [\Delta L(x)]^2 \rangle)\}$$

At any non-zero temperature, in agreement with the simple physical argument given above, it is straightforward to show that $\langle [\Delta L(x)]^2 \rangle \sim A|x|$ for large $|x|$, where A is a complicated measure of the magnitude of the transverse stripe fluctuations. It is important to note that A is dominated by short-wavelength transverse fluctuations, and is insensitive to details of their quantum dynamics. At precisely $T = 0$, for technical reasons that are not important for present purposes, the dephasing effect is somewhat more subtle, and in fact $\langle [\Delta L(x)]^2 \rangle \sim A\hbar\omega \log|x|$, which implies that \bar{V} falls as a power of $|x|$ as opposed to the exponential fall-off at non-zero T . These expressions, which can readily be extended to higher order in perturbation theory and higher order in the cumulant expansion, capture the essential general point of the physics—that the effective coupling between CDWs vanishes except in a narrow 'surface' region at the ends of the stripes, and hence can be ignored in the thermodynamic limit.

The effect of Josphenson coupling between stripes may be analysed in the same way. To first order in J , the effective action is proportional to:

$$\langle J \rangle \approx J_0 \exp\{(\alpha^2/2) \langle [\Delta_j Y]^2 \rangle\} \quad (8)$$

Hence the superconducting coupling is strongly enhanced by the transverse stripe fluctuations. (There is a similar enhancement of the CDW coupling, V , but it is overwhelmed by the dephasing effect.) Physically, this enhancement reflects the fact that the mean value of J is dominated by regions where neighbouring stripes come close together so that $\langle J \rangle$ is very much larger than the median. From equation (1) it can be seen that, when $K_c > 1/2$, the pair susceptibility on an individual stripe diverges as $T \rightarrow 0$ and hence, for non-zero J , the smectic phase is always globally superconducting below a finite (Kosterlitz–Thouless) ordering temperature, $T_c \sim (\langle J \rangle \Delta_s)^{K_c/(2K_c-1)}$. Because of the broken rotational symmetry of this phase, all that can be said about the symmetry of the superconducting state is that it is singlet; its symmetry is necessarily a mixture of 's-wave' and 'd-wave'. On the other hand, for $K_c < 1/2$ and $\langle J \rangle$ sufficiently small, the system remains a (quantum critical) non-Fermi liquid all the way to $T = 0$. Although such quantum critical phases are common in one dimension¹⁰, where they are often called 'Luttinger liquids', we believe this is the first theoretically well justified example in two dimensions.

To complete the physical picture of the quantum smectic, we construct a global phase diagram, shown schematically in Fig. 2, by considering the possible zero and finite temperature phase transitions from the smectic state to states with other symmetries. This can be done, to a large extent, on the basis of general considerations

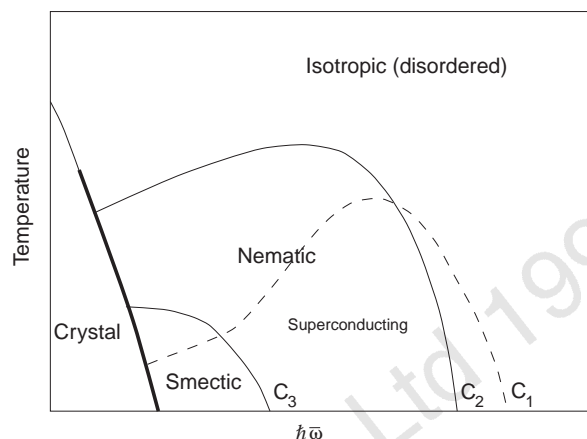


Figure 2 Phase diagram for $K_c > 1/2$. Here $\hbar\omega$ is a measure of the magnitude of the transverse zero-point fluctuations of the stripes. Thin lines represent continuous transitions, and the thick line is a first-order transition. The dashed line is the superconducting T_c . The symbols C_j label various quantum-critical points. Depending on microscopic details, the positions of C_1 and C_2 could be interchanged.

of symmetry and by analogy with the phase diagram of conventional liquid crystals; the argument relies on nothing more than the existence (and electronic character) of the quantum smectic phase.

Along the $T = 0$ axis of the figure, the phases evolve as $\hbar\omega$ is varied. Starting from the smectic phase:

(1) To the left, as the system becomes progressively more 'classical', there is a (first-order) phase transition to a crystalline state, in which the phases of the CDWs on neighbouring stripes are locked, the transverse stripe fluctuations become the phonons of a fully ordered crystal, superconducting order is destroyed, and the system becomes globally insulating.

(2) To the right, as the system becomes more quantum and, in particular, when the r.m.s. magnitude of the transverse fluctuations of the stripes becomes comparable to their spacing, there is a $T = 0$ transition to a quantum nematic phase. This transition is driven by dislocations which destroy the stripe positional ordering at long distances. We generally expect this transition to be continuous. This implies that, for $K_c > 1/2$, the superconducting order must continue across the smectic to nematic phase boundary. Similarly, in the case $K_c < 1/2$, the Luttinger liquid behaviour must persist across the phase boundary.

(3) At still larger $\hbar\omega/V$, there must be a transition to an isotropic phase. Landau theory suggests that the nematic to isotropic transition should be continuous in two spatial dimensions, although it is first-order in three.

(4) For $K_c > 1/2$, there are two possible schemes for the termination of the high-temperature superconducting order with increasing $\hbar\omega$: If the nematic region of the phase diagram is narrow, so that significant local stripe correlations survive into the isotropic phase, then the superconducting state could survive until some larger value of $\hbar\omega$, as shown in Fig. 2; in this case, the superconducting state will have a pure symmetry ('s' or 'd') where it extends into the isotropic phase. Otherwise, the high-temperature superconducting phase could terminate at a critical point within the nematic phase. In either case, beyond this point, the ground state is a (possibly) anisotropic Fermi liquid (similar to a conventional metal) or, if there remain sufficient residual interactions, a low-temperature superconductor. A highly schematic view of the local stripe order in these various phases is shown in Fig. 3.

Except for the choices among the possible schemes described above, and so long as the phase transitions are continuous, the topology of the phase diagram is constrained to be as shown in Fig. 2 for the case $K_c > 1/2$. At high enough temperature, there must be a

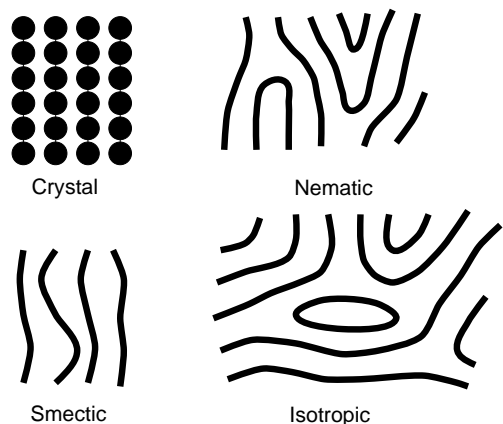


Figure 3 Schematic view of the local stripe order in the various phases discussed in the text. Here, we have assumed that the stripes maintain their integrity throughout, although in reality they must certainly become less and less well defined as the system becomes increasingly quantum, until eventually they are not the correct variables for describing the important correlations in the system. Heavy lines represent liquid-like stripes, along which the electrons can flow, whereas the filled circles represent pinned, density-wave order along the stripes. The stripes are shown executing more or less harmonic oscillations in the smectic phase. Two dislocations, which play an essential role in the smectic-to-nematic phase transition, are shown in the view of the nematic phase.

transition from a smectic to an isotropic (symmetric) phase. As at zero temperature, the smectic order is destroyed in a sequence of two transitions: (1) a dislocation unbinding transition to an “Ising nematic” phase¹⁸ which has short-range positional order but breaks four-fold rotational symmetry, and (2) a transition to the isotropic state. The superconducting T_c rises with $\hbar\omega$ through the smectic and nematic phases, reflecting the enhancement of the Josephson coupling, J , by transverse stripe fluctuations; it decreases at larger $\hbar\omega$ following the isotropic to nematic phase boundary, as we expect that the stripes lose their local integrity far into the isotropic phase. A further detail is that both the crystalline and smectic regions are actually a series of commensurate phases at $T = 0$, and a complicated pattern of commensurate and incommensurate phases for $T \neq 0$. Whereas the commensurate smectic has true positional long-range order, the incommensurate smectic will have only power-law correlations, and there is no true broken translational symmetry—only quasi-long-ranged positional order. If any of the phase transitions were discontinuous (first-order), the character of the phase diagram would change. An important and interesting possibility is that C_1 could be replaced by a line of first-order phase transitions, extending to finite temperature in either the nematic or isotropic regions of the phase diagram.

As mentioned above, crystals do not have the full rotational symmetry of free space. A crystal field with two-fold symmetry would change the nematic-to-isotropic phase transition into a crossover, which nevertheless would be quite sharp if the field is small. We note that our analysis could also be applied to systems with low-energy spin degrees of freedom by considering the most general model of the one-dimensional electron gas with or without a charge gap¹⁰.

What are the experimental signatures of the electronic liquid-crystal phases? The most direct would come from peaks in the static and dynamic, spin and charge structure factors, measured by neutron and X-ray scattering. Long-range order transverse to the stripes is indicated by a Bragg peak for which the component, q_x , of the wavevector along the stripe direction is equal to zero. There are additional peaks with $q_x \neq 0$ corresponding to CDW ordering along the stripes—Bragg peaks in the case of the crystalline phase, and power-law singularities for the smectic. In practice, the latter may be

of low intensity and difficult to observe. However, the electrical conductivity allows an unambiguous distinction to be made between the insulating crystalline phase and the metallic smectic phase. In the nematic phase near to the smectic phase boundary, sharp peaks corresponding to smectic order with a long but finite correlation length should also be observable in the static structure factor. In addition, the electronic properties should be strongly anisotropic, as this phase breaks four-fold rotational symmetry, even in a nominally tetragonal material. This analysis is complicated by the effects of quenched disorder, which always leads to a rounding of the Bragg peaks in two dimensions, even in the crystalline phase.

There is strong direct experimental evidence of electronic liquid-crystal phases in the copper oxide superconductors. Neutron-scattering experiments by Tranquada *et al.*^{11,12} have found static peaks, corresponding in incommensurate spin and charge stripe order, in $\text{La}_{1.6-x}\text{Nd}_{0.4}\text{Sr}_x\text{CuO}_4$. The stripes are along the CuO direction and the material is simultaneously a bulk superconductor. The peaks have a small but finite width which is consistent with a nematic stripe phase in an orientating potential. However, because of the presence of quenched disorder in these materials, the peaks could possibly arise from a disrupted smectic phase. In this material, the orientation of the oxygen octahedra produces a two-fold symmetry-breaking potential that drives the material either into or close to the smectic phase, and freezes the dynamics. In $\text{La}_{2-x}\text{Sr}_x\text{CuO}_4$ there are similar incommensurate peaks in the magnetic neutron-scattering factor at about the same position in \mathbf{k} -space, but they are inelastic^{13–16}; that is, there are dynamically fluctuating analogues of the stripe phases seen in $\text{La}_{1.6-x}\text{Nd}_{0.4}\text{Sr}_x\text{CuO}_4$. Here the two-fold lattice potential is, itself, dynamical. Neutron-scattering experiments on underdoped $\text{YBa}_2\text{Cu}_3\text{O}_{7-\delta}$ also have found dynamical incommensurate peaks^{19,20}, corresponding to low-energy dynamical stripe fluctuations. □

Received 21 July 1997; accepted 31 March 1998.

- Kivelson, S. A. & Emery, V. J. Topological doping. *Synth. Met.* **80**, 151–158 (1996).
- Zaanen, J. & Gunnarsson, O. Charged magnetic domain lines and the magnetism of high T_c oxides. *Phys. Rev. B* **40**, 7391–7394 (1989).
- Schulz, H. J. Incommensurate antiferromagnetism in the 2-dimensional Hubbard model. *Phys. Rev. Lett.* **64**, 1445–1448 (1990).
- Kivelson, S. A. & Emery, V. J. in *Strongly Correlated Electron Materials: The Los Alamos Symposium 1993* (eds Bedell, K. S., Wang, Z., Meltzer, D. E., Balatsky, A. V. & Abrahams, E.) 619–650 (Addison-Wesley, Redwood City, 1994).
- Nayak, C. & Wilczek, F. Populated domain walls. *Phys. Rev. Lett.* **78**, 2465–2468 (1997).
- Castro-Neto, A. H. Superconducting phase coherence in striped cuprates. *Phys. Rev. Lett.* **78**, 3931–3934 (1997).
- Devreese, J. T., Evrard, R. P. & van Doren, V. E. (eds) *Highly Conducting One-Dimensional Solids* (Plenum, New York, 1979).
- Chaikin, P. M. & Lubensky, T. C. *Principles of Condensed Matter Physics* (Cambridge Univ. Press, 1995).
- Emery, V. J., Kivelson, S. A. & Zachar, O. Spin-gap proximity effect mechanism of high-temperature superconductivity. *Phys. Rev. B* **56**, 6120–6147 (1997).
- Emery, V. J. in *Highly Conducting One-Dimensional Solids* (eds Devreese, J. T., Evrard, R. P. & van Doren, V. E.) 247–303 (Plenum, New York, 1979).
- Tranquada, J. M. *et al.* Evidence for stripe correlations of spins and holes in copper oxide superconductors. *Nature* **375**, 561–563 (1995).
- Tranquada, J. M. *et al.* Coexistence of, and competition between, superconductivity and charge-stripe order in $\text{La}_{1-x}\text{Nd}_x\text{Sr}_x\text{CuO}_4$. *Phys. Rev. Lett.* **78**, 338–341 (1997).
- Cheong, S.-W. *et al.* Incommensurate magnetic fluctuations in $\text{La}_{1-x}\text{Sr}_x\text{CuO}_4$. *Phys. Rev. Lett.* **67**, 1791–1794 (1991).
- Mason, T. E., Aeppli, G. & Mook, H. A. Magnetic dynamics of superconducting $\text{La}_{1.86}\text{Sr}_{0.14}\text{CuO}_4$. *Phys. Rev. Lett.* **68**, 1414–1417 (1992).
- Thurston, T. R. *et al.* Low-energy incommensurate spin excitations in superconducting $\text{La}_{1.85}\text{Sr}_{0.15}\text{CuO}_4$. *Phys. Rev. B* **46**, 9128–9131 (1992).
- Yamada, K. *et al.* Direct observation of a magnetic gap in superconducting $\text{La}_{1.85}\text{Sr}_{0.15}\text{CuO}_4$ ($T_c = 37.3$ K). *Phys. Rev. Lett.* **75**, 1626–1629 (1995).
- Pokrovsky, V. L., Talapov, A. L. & Bak, P. in *Solitons* (eds Trullinger, S. E., Zakharov, V. E. & Pokrovsky, V. L.) 71–127 (North Holland, Amsterdam, 1986).
- Abanov, A. *et al.* Phase diagram of ultrathin ferromagnetic films with perpendicular anisotropy. *Phys. Rev. B* **51**, 1023–1038 (1995).
- Tranquada, J. M. Charge stripes and spin correlations in copper oxide superconductors. *Physica C* **282–287**, 166–169 (1997).
- Dai, P., Mook, H. A. & Dogan, F. Incommensurate magnetic fluctuations in $\text{YBa}_2\text{Cu}_3\text{O}_{6.6}$. *Phys. Rev. Lett.* **80**, 1738–1741 (1998).

Acknowledgements. We thank J. Tranquada for discussions and V. Pokrovskii for comments. This work was supported in part by the NSF at UCLA, UIUC and ITP-UCSB; and in part by the Division of Materials Science, US DOE, at Brookhaven. Two of us (E.E. and S.K.) were participants at the ITP Program on Quantum Field Theory in Low Dimensions.

Correspondence and requests for materials should be addressed to V.J.E. (e-mail: emery@cmth.phy.bnl.gov).